Bulletin of the Geological Society of Malaysia, Volume 74, November 2022, pp. 43 - 53
DOI: https://doi.org/10.7186/bgsm74202203

Drained shear strength parameters of saprock from a weathering profile over porphyritic biotite granite at Km 31 of the Kuala Lumpur - Karak Highway, Peninsular Malaysia

John Kuna Raj

No. 83, Jalan Burhanuddin Helmi 2, Taman Tun Dr. Ismail, 60000 Kuala Lumpur, Malaysia
Author email address: jkr.ttdi.tmc@gmail.com

Abstract: Three broad zones can be differentiated at the weathering profile; an upper, 9.4 m thick, pedological soil (zone I), an intermediate, 31.7 m thick, saprock (zone II) and the bottom bedrock (zone III). The saprock (zone II) comprises gravelly silty sands that distinctly preserve the minerals, textures and structures of the original bedrock and can be separated into sub-zones II A, II B, II C and II D based on differences in preservation of relict structures and content of litho-relicts (core-boulders). To characterize the drained strength of saprock, samples were collected from sub-zones II B, II C and II D, and their physical and soil index properties determined before consolidated, drained triaxial tests were carried out on remolded specimens. Three individual specimens from each sub-zone were consolidated for 24 hours and compressed at a rate of 0.152 mm/min under confining pressures of 138 kPa, 207 kPa and 276 kPa. The tests yielded effective cohesions (c') of 30.6 kPa, 9.5 kPa, and 20.2 kPa, and friction angles of 33.2°, 31.4° and 34.4°, for the samples from sub-zones II B, II C and II D, respectively. Regression analyses show effective cohesions (c') to increase with increasing moisture contents retained at 4.19 pF (1,500 kPa) suction; a feature indicating the influence of negative pore water pressures (matric suction). Regression analyses also show effective friction angles to increase with increasing sand, and sand and gravel, contents; a feature indicating increased inter-locking and resistance to displacement of coarse particles during shear. It is concluded that the saprock is characterized by an average effective cohesion of 14.5 kPa, and friction angle of 34.3°; these parameters influenced by the moisture content retained at 1,500 kPa suction, and the sand and gravel contents.

Keywords: Consolidated drained triaxial tests, saprock, gravelly silty sand, effective cohesion, effective friction angle

INTRODUCTION

Weathering profiles are found in most parts of the world and show variable patterns and thicknesses for the rates, depths and courses of weathering are influenced by several factors, including climatic, biotic, geomorphic, site, geologic and chronologic ones (Thomas, 1974). As weathering occurs *in situ*, the weathered materials accumulate at the sites of formation and give rise to thick mantles of weathered materials (or regolith) over bedrock. The regoliths show variations in the extent of preservation of the minerals, textures and structures of the original bedrock; the vertical sequence of materials of different composition extending up to the ground surface from the unaltered bedrock below known as the weathering profile (Dearman, 1974; Raj, 2009).

Deep weathering profiles are found in Peninsular Malaysia as a result of favorable tectonic and environmental settings that have facilitated prolonged and pervasive chemical weathering throughout most of the Cenozoic Era (Raj, 2009). The earth materials in these weathering profiles are classified as 'residual soils' in geotechnical literature and said to have characteristics that are quite different from those of 'transported or sedimentary soils' (Tan & Gue, 2001; Wesley, 2009). As unconfined groundwater tables in the hilly to mountainous terrain of Peninsular Malaysia are located at depth (several tens of meters below the ground surface), the 'residual soils' are also known as 'unsaturated soils' that are characterized by negative pore water pressures (or suction) (Faisal *et al*., 2005).

'Residual soils' are said to be of a very heterogeneous nature which makes the sampling and testing of representative parameters difficult, whilst their usually high permeability makes them susceptible to rapid changes in material properties when subjected to changes of external hydraulic condition (Tan & Gue, 2001). The shear strength parameters of 'residual soils' in tropical areas are also said to be generally higher than those of 'sedimentary soils' (Wesley, 2009). It has thus been pointed out that it is rare for the undrained strength of 'residual soils' to be less than about 75 kPa, whilst their effective friction angles are generally above 30° with significant values of effective cohesion (Wesley, 2009).

In a review of 'residual soils' over granite in Peninsular Malaysia, it was concluded that "the degree of weathering process and clay content" have a significant influence on their engineering properties; the properties being similar at the same subsurface level, but varying with depth (Salih, 2012). The review noted that the effective cohesion of these soils ranged from 7 to 77 kPa, whilst the effective friction

0126-6187; 2637-109X / Published by the Geological Society of Malaysia.

angle was between 17° and 40°. The review also pointed out that there was very limited published data in Malaysia on the determination of shear strength parameters from consolidated drained triaxial tests.

Consolidated drained triaxial tests on saprolite samples from a residual soil over granite were reported to yield an effective cohesion of 10 kPa, and friction angle of 28.1° (Mohd Raihan *et al.*, 1998). Consolidated drained triaxial tests on a remolded gravelly silt (from a depth of 1.5 to 2.5 m in a residual soil over granite) furthermore, were reported to yield effective cohesions of 8 to 9 kPa, and friction angles of 28° to 30° (Salih & Kassim, 2012). Consolidated drained triaxial tests on a clayey gravel (from saprolite in a residual soil over granite), remolded at 100, and 200, kPa, yielded effective cohesions of 8.13, and 9.04, kPa, and friction angles of 28.17°, and 29.79°, respectively (Salih & Ismael, 2019). Similar triaxial tests on a silty gravel (from the same saprolite), remolded at 100, and 200, kPa, furthermore, yielded effective cohesions of 1.12, and 1.42, kPa, and friction angles of 31.02°, and 32.57°, respectively (Salih & Ismael, 2019).

In the course of a study on the characterization of weathering profiles in Peninsular Malaysia was investigated the profile over porphyritic biotite granite at Km 31 of the Kuala Lumpur - Karak Highway (Raj, 1983). The characterization of this profile based on field mapping and differentiation of morphological zones and sub-zones followed by laboratory determination of their physical and soil index properties has been earlier discussed (Raj, 1985). The soil-moisture retention characteristics of earth materials in the said weathering profile as well as their saturated hydraulic conductivity have also been earlier discussed (Raj, 2010; 2021). This paper discusses determination of the drained shear strength parameters of saprock (zone II) from the weathering profile and is based on consolidated drained triaxial tests of remolded samples collected at three different depths.

METHODOLOGY

The investigated weathering profile is located at the slope cut at Km 31 of the Kuala Lumpur - Karak Highway and was exposed during earthworks for construction of the Highway (Figure 1). Field mapping was first carried out to visually differentiate morphological zones and sub-zones, followed by the collection of constant volume samples at various depths to determine the physical and soil index properties of the earth materials present (Raj, 1985).

Samples for triaxial tests were collected with stainless steel tubes of 21.6 cm length and 4.1 cm internal diameter at three different depths in the saprock (Zone II) (Figure 2). The tubes had a constant wall thickness of 0.2 cm except towards one end, where the wall tapered to provide a cutting edge. Prior to sampling, the tubes were externally greased to facilitate entry, whilst materials on the slope were removed to a depth of some 0.5 m to minimize surface effects. Each of the sampling tubes was driven into the soil by gently hammering on a block of wood placed on its top and then

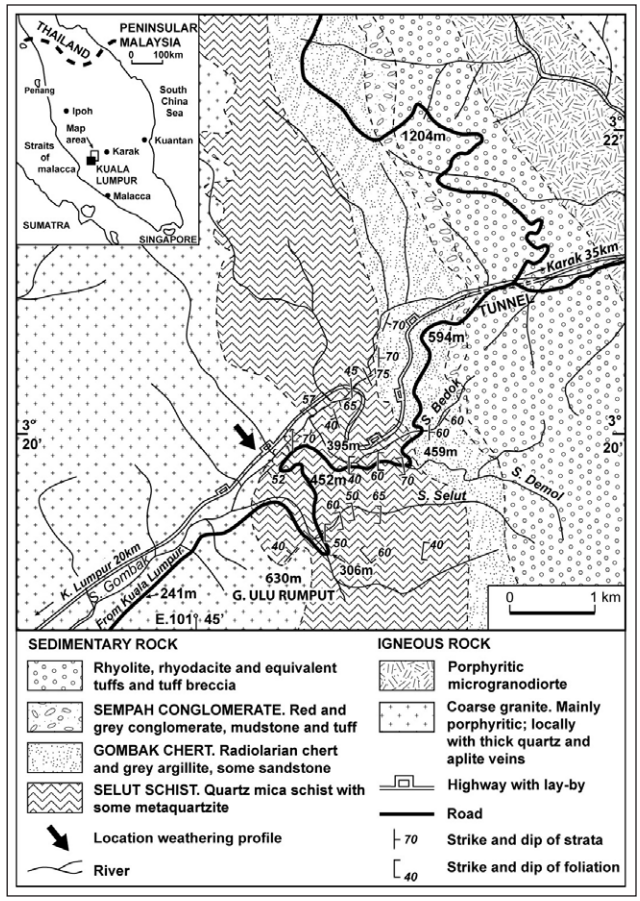

Figure 1: Geology map of the Genting Sempah area, Pahang and Selangor (Haile *et al.*, 1977).

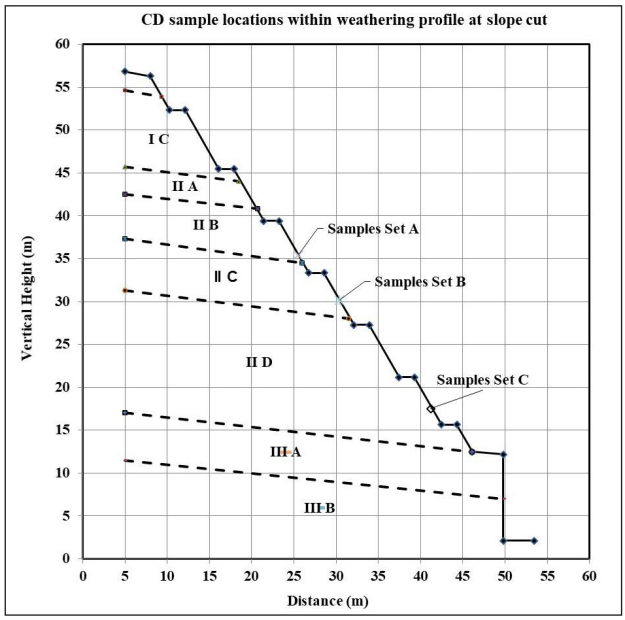

Figure 2: Locations of sample sets in the weathering profile.

retrieved by removing the surrounding, and underlying, soil. The ends of the sample were trimmed and sealed with solidified wax to prevent moisture loss before being taken to the laboratory. Three tube samples were collected adjacent to one another at every sampling site together with samples for determination of physical and soil index properties.

A mechanical core extruder was used to retrieve the individual samples which mostly disaggregated on extrusion (except for one sample). Remolded specimens were then prepared by compacting the disaggregated material (to field density and moisture content) in a constant volume mold of 3.81 cm internal diameter and 7.62 cm height.

Individual specimens were weighed, capped at their top, and bottom, ends with perspex, and porous, discs, respectively, and then enclosed in a close fitting rubber membrane. The specimens were sealed with O-rings placed around the top and bottom discs and then mounted on the pedestal of the triaxial cell. The enclosing perspex cylinder was screwed onto the base, filled with distilled water and placed under a specified cell pressure according to standard procedure (Bishop & Henkel, 1957). Each specimen was allowed to consolidate under the specified pressure for a period of 24 hours; a 10 ml burette attached to the open drainage valve to allow recognition of any volume change.

At the end of consolidation (24 hours), the specimens were compressed at a constant rate of 0.152 mm/min (0.006 in/min); load gauge readings on the proving ring being recorded at specified compression gauge readings. Compression was usually stopped when an axial strain of 20% was reached; the cell pressure then reduced and water removed to describe the sample after test. Graphs of deviator stress versus axial strain were then plotted; the total compressive stresses at the maxima of the deviator stress-strain curves used to construct Mohr circles and Mohr-Coulomb failure envelopes.

It is to be noted that saturation of specimens prior to consolidation (with the use of back-pressure) was not carried out as restricted time periods were available for use of the laboratory equipment. In this respect, it is to be noted that the high back pressures required for saturation can increase the moisture content and saturation level which causes a reduction in the effective cohesion (Salih, 2012). It has also been said that the effective friction angle is not affected by soil saturation (Salih, 2012), whilst the measured values of effective cohesion are very small (Brand, 1982).

Three individual samples of each set were tested under confining cell pressures of 138, 207, and 276, kPa, as multi-stage testing of single samples is said to produce misleading results (Tan & Gue, 2001). The deviator stress ($\sigma1 - \sigma3$) versus axial strain for each of the individual tests was plotted and a Mohr circle then drawn to represent the state-of-stress at the peak value. The values of $pf = [(\sigma1 + \sigma3)/2]$ and $qf = [(\sigma1 - \sigma3)/2]$ corresponding to the peaks of the stress-strain curves of the individual specimens from each sample set were then plotted. The line drawn through the points is known as the K_f *line*; its gradient ($\acute{\alpha}$) and intercept (a) used to calculate the shear strength parameters of effective cohesion (c') and effective angle of friction (φ') (Lambe & Whitman, 1973).

It is to be noted that the proving rings and other equipment employed in the triaxial tests were calibrated in Imperial (or British) System units. Correlation factors were thus applied to the original measurements in order to convert them to SI (System International) units.

GEOLOGICAL SETTING OF INVESTIGATED WEATHERING PROFILE

The investigated weathering profile is developed over a porphyritic biotite granite that forms part of the eastern lobe of the Late Triassic (199 - 210 Ma) Kuala Lumpur Granite (Ng, 1992). The bedrock continues to outcrop to the west over a distance of about 10 km, but to the east, is in contact with a sequence of schists, sedimentary and volcanic rocks, that occur as a roof pendant within the Main Range Granite (Haile *et al.*, 1977).

The granitic bedrock exposed at the cut is strongly jointed and cut by a number of moderately to steeply dipping faults of variable strike. A number of epidote and quartz feldspar veins with tourmaline as well as aplite and leucocratic microgranite dykes are also seen within the bedrock. The grey bedrock is medium to coarse grained and usually porphyritic with large alkali feldspar phenocrysts (up to 4 cm in length). The essential minerals are quartz, alkali feldspar, plagioclase feldspar and biotite, whilst the accessory minerals include apatite, tourmaline and zircon. Quartz occurs as anhedral crystals, filling interstices in the groundmass and sometimes forms small phenocrysts. The alkali feldspars include microcline, orthoclase and perthite, and occur both as phenocrysts and as fine to medium grained crystals in the groundmass. The alkali feldspars sometimes contain quartz, biotite and plagioclase inclusions. The plagioclase feldspars, of albite to andesine composition, are usually found as euhedral to subhedral, fine to medium grained crystals in the groundmass and are often sericitized. The biotites occur as fine to medium grained, generally euhedral crystals and found both as disseminated grains and as aggregates in the bedrock. Close to the faults, hydrothermal alteration of the plagioclase feldspar and biotite grains has occurred.

MORPHOLOGICAL ZONATION OF WEATHERING PROFILE

Vertical and lateral variations in the extent of preservation of the minerals, textures and structures of the original bedrock allow differentiation of three broad zones at the weathering profile, i.e. an upper pedological soil (zone I), an intermediate saprock (zone II), and the underlying bedrock (zone III). The zones are developed about parallel to the overlying ground surface and are of maximum thickness below the ridge crest but thin towards the valley sides. Descriptions of the different morphological zones (and

sub-zones) are summarized in Table 1 and schematically shown in Figure 3 (Raj, 1985). *In situ* development of the saprock (zone II) indicates weathering of bedrock due to gradual lowering of an unconfined groundwater table which is now located at its' (zone II) bottom.

The pedological soil (zone I) is 9.4 m thick with the A and B soil horizons (solum) consisting of friable to firm, sandy clay, whilst the C horizon (saprolite) comprises stiff to very stiff, clayey sand with indistinct to distinct relict granitic textures (Table 1). The saprock (zone II) is 31.7 thick and consists mainly of gravelly silty sands that indistinctly to distinctly preserve the minerals, textures and structures of the original granite; the degree of preservation increasing with depth. This Zone can be separated into four sub-zones; the top two (II A and II B) devoid of core-boulders, whilst the lower two, II C and II D, have some (<40% by area), or many (>70% by area), core-boulders, respectively (Table 1). The bedrock (zone III) is a continuous granite outcrop with weathering (marked by narrow to broad, strips of gravelly silty sand) along, and between, discontinuity planes (III A), or only along discontinuity planes (III B).

In terms of rock mass weathering grades as proposed by IAEG (1981) and GSL (1990), the pedological soil (zone I) would be classified as rock mass weathering grade VI and the bedrock zone (zone III) as weathering grade II. In view of the litho-relicts (core-boulders) present, sub-zones

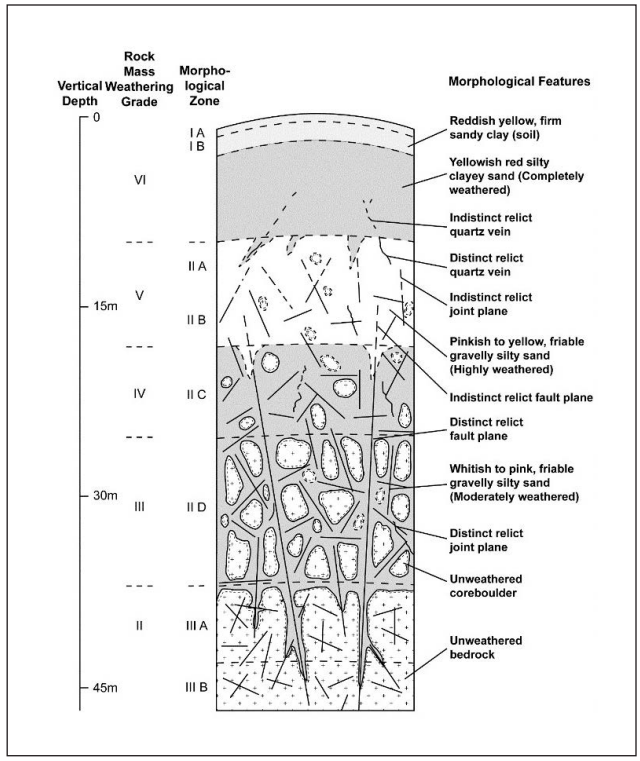

Figure 3: Schematic sketch of morphological features in the weathering profile.

Table 1: Field descriptions of morphological zones and sub-zones (Raj, 1985).

Sub-zone	Thickness (m)	Field Description
I A	0.6	Brownish yellow, sandy clay, porous, soft; friable dry; sub-angular blocky; many roots; boundary irregular, diffuse.
I B	1.0	Reddish yellow, firm, sandy clay; friable, dry; sub-angular blocky; some roots; boundary wavy, sharp.
I C	7.8	Yellowish red, stiff to very stiff, clayey sand with some reddish yellow mottles; friable, dry; sub-angular blocky; indistinct to distinct relict bedrock texture; a few distinct relict quartz veins; boundary irregular, sharp.
II A	4.5	Yellowish red, friable, gravelly, silty sand with red & white mottles; thin bands & wedges of yellowish red clayey sand; distinct relict bedrock texture & quartz veins; some indistinct relict joint planes; boundary, irregular, diffuse.
II B	6.0	White, friable, gravelly silty sand with bands of yellowish red, gravelly silty sand; distinct relict bedrock texture, quartz veins & joint planes; boundary, irregular, diffuse.
II C	7.3	Pinkish to yellowish red, friable, gravelly silty sand; distinct relict bedrock texture, quartz veins, joint & fault planes; some fresh core-boulders (20 - 40% by area); boundary, irregular, diffuse.
II D	13.9	Dominantly partly weathered to fresh, rounded core-boulders (>70% by area) surrounded by thin to broad bands of whitish, friable, gravelly silty sand with distinct relict bedrock textures, quartz veins, joint & fault planes; boundary, irregular, sharp.
III A	5.0	Continuous granite outcrop with effects of weathering (including alteration of feldspars & formation of gravelly silty sand) along & between joint & fault planes; boundary, broken, diffuse.
III B	>2.0	Continuous granite outcrop with effects of weathering along joint & fault planes only.

II D, and II C, constitute rock mass weathering grades III and IV respectively, whilst sub-zones II A and II B would be classified as weathering grade V (Figure 3).

RESULTS

Descriptions of sampled earth materials

The samples were collected at different depths in saprock in sub-zones II B, II C and II D (Figure 2) and thus retain the original granitic bedrock texture (Table 2). Minor variations in composition, however, are seen; the clay fractions all characterized by the presence of kaolinite with illite additionally present in Sets B and C. The coarse grained fractions of all samples consist of angular quartz grains, sericite flakes and altered (kaolinized) feldspar grains; fresh feldspar fragments also present in the Set C samples (Table 2).

Physical properties of sampled earth materials

As the samples were collected at different depths, there are some differences in their physical properties (Table 3). Constant volume samples show their dry unit weights to range between 12.58 and 14.10 kN/m^3, and their dry densities from 1,282 to 1,437 kg/m^3. Porosity is somewhat variable with values of 45.2% to 50.7%, whilst the specific gravity of soil particles is between 2.60 and 2.62. Moisture contents show a limited variation from 7.0% to 8.9%; the degrees of saturation ranging from 19.5% to 22.5% (Table 3).

Soil index properties of sampled earth materials

Grain size distributions show some variations; set C having the largest sand content of 72%, whilst sets A and B have contents of 61%, and 51%, respectively (Table 4). Gravel contents are low; sets A, B and C having contents of 10%, 7%, and 8%, respectively. Set C has the largest coarse grained fraction with a combined sand and gravel content of 80% while sample sets A and B have combined contents of 71%, and 68%. Silt contents are variable; set C with 16% and sets A and B with 26%, and 23%, respectively. Clay contents are rather limited with sets A, B and C having contents of 3%,

Table 2: Descriptions of sampled earth materials.

Set Samples	Sub-zone	Vertical Depth	Description
Set A (1,2,3)	II B	20.86 m	Pinkish to yellowish, friable, gravelly silty sand with distinct relict bedrock texture. Very highly weathered granite. Coarse fraction of quartz grains & sericite flakes with some kaolinized feldspar fragments. Clay fraction of kaolinite.
Set B (4,5,6)	II C	31.29 m	Pinkish to grey, friable, gravelly silty sand with distinct relict bedrock texture. Highly weathered granite. Coarse fraction of quartz grains & sericite flakes with many altered feldspar fragments. Clay fraction of kaolinite with some illite.
Set C (7,8,9)	II D	41.93 m	White to light grey, friable, gravelly silty sand with distinct relict bedrock texture. Moderately weathered granite. Coarse fraction of quartz grains & sericite flakes with many altered, & some fresh, feldspar fragments. Clay fraction of kaolinite & illite.

Table 3: Physical properties of sampled earth materials.

Set Samples	Dry Unit Weight (kN/m^3)	Dry Density (kg/m^3)	Specific Gravity Particles	Porosity (%)	Void Ratio	Moisture Content (%)	Degree Saturation (%)
Set A (1.2.3)	12.59	1,283	2.600	50.6	1.03	8.9	22.5
Set B (4,5,6)	12.58	1,282	2.600	50.7	1.03	7.7	19.5
Set C (7,8,9)	14.10	1,437	2.620	45.2	0.82	7.0	22.1

Table 4: Soil index properties of sampled earth materials.

Set Samples	Sub-zone	Gravel (%)	Sand (%)	Silt (%)	Clay (%)	Gravel & Sand (%)	Plastic Limit (%)
Set A (1.2.3)	II B	10	61	24	4	71	42.5
Set B (4,5,6)	II C	17	51	23	9	68	41.7
Set C (7,8,9)	II D	8	72	16	4	80	26.7

9% and 4%, respectively (Table 4). Plastic limits are variable with sets A, B and C having values of 42.5%, 41.7%, and 26.7%, respectively (Table 4). Liquid limits, however, could not be determined as the large silt contents prevented proper use of the standard Casagrande grooving tool.

Deviator stress versus axial strain curves

Plots of deviator stress (σ_1 - σ_3) versus axial strain for all specimens show a similar pattern with curves that initially rise steeply (to about 3% strain) and then gradually (to about 8% strain) before levelling off and generally dropping (Figures 4 to 6). It is interesting to note that these stress-strain curves are very similar to those of consolidated drained tests on loose sand (and normally consolidated clay) where the curves gradually rise until a peak value is reached and then become horizontal (Lambe & Whitman, 1973).

It is to be noted that only one sample (A 1) remained intact after extrusion from the sampling tube; the other samples disaggregating and having to be remolded (or recompacted). The deviator stress versus axial strain plots of the undisturbed and remolded samples of Set A, however, show little difference (Figure 6).

The specimens after testing developed barrel shapes (i.e. shortening and bulging around the waist) with the formation of diagonal shear planes. The peaks of the stress-strain curves thus represent the maximum stress that the specimens can support. Results of the consolidated drained triaxial tests in terms of the cell pressure (σ_3) and deviator stress (σ_1 - σ_3) at peak axial strain are listed in Table 5.

Drained shear strength parameters

Plots of the values of *pf* = [(σ1 + σ3)/2] and *qf* = [(σ1 - σ3)/2] of individual samples and the drawing of K_f *lines* (after Lambe & Whitman, 1973) allowed for calculation of

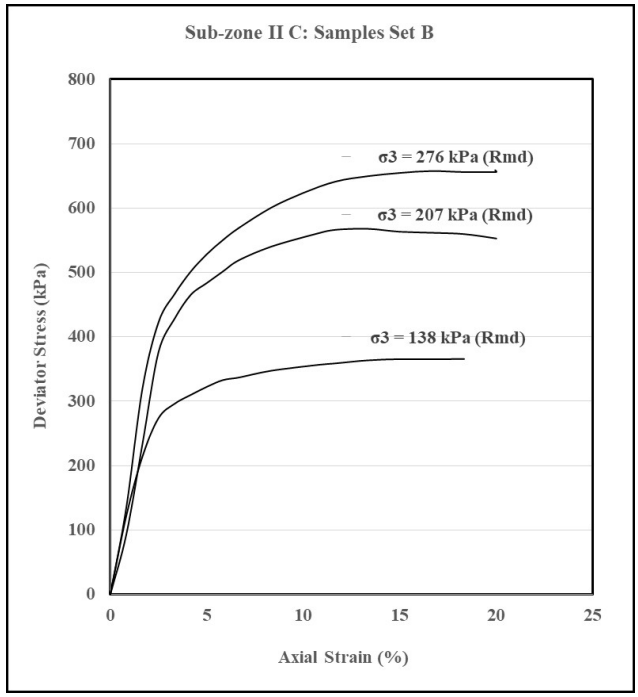

Figure 5: Deviator stress versus axial strain - Set B samples (sub-zone II C).

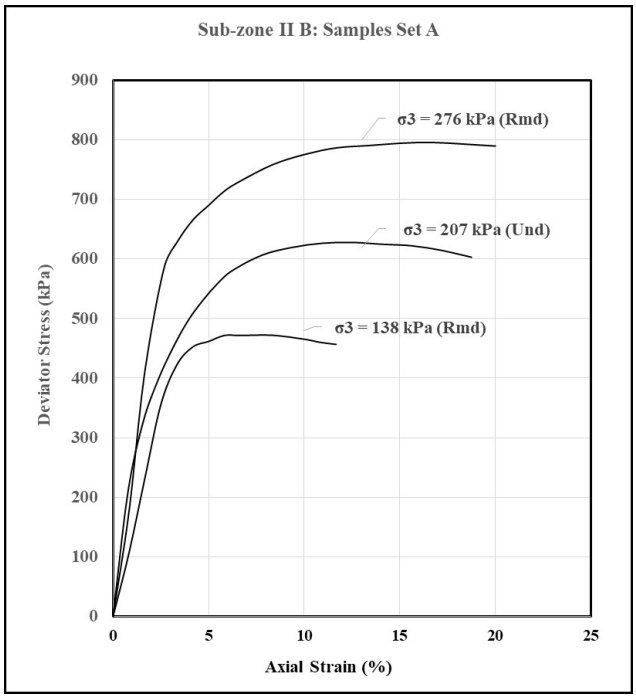

Figure 4: Deviator stress versus axial strain - Set A samples (sub-zone II B).

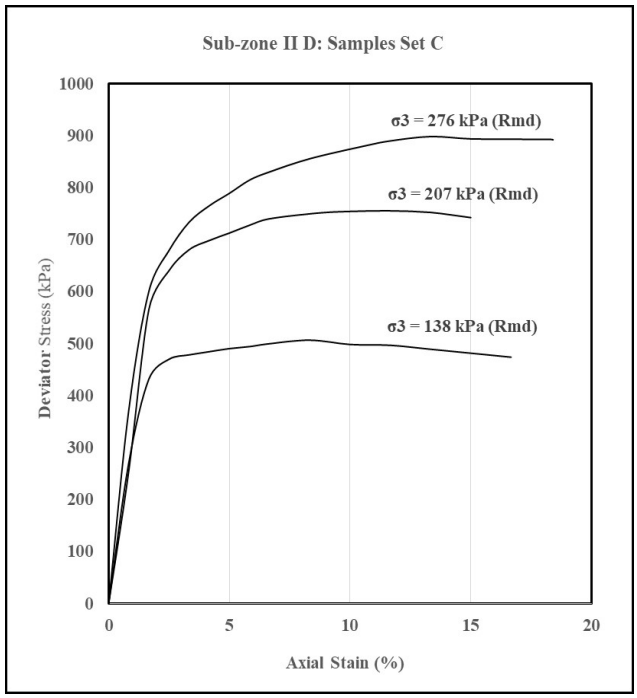

Figure 6: Deviator stress versus axial strain - Set C samples (sub-zone II D).

Table 5: Results of consolidated, drained triaxial tests.

Set	Sample No.	Sub-zone	Sample Type	Cell Pressure (kPa)	Peak Axial Strain (%)	Peak Deviator Stress (kPa)
A	1	II B	Undisturbed	207	10.9	630.2
A	2	II B	Remolded	276	16.7	806.0
A	3	II B	Remolded	138	8.33	472.3
B	4	II C	Remolded	276	16.7	657.8
B	5	II C	Remolded	138	15.0	365.8
B	6	II C	Remolded	207	13.3	567.9
C	7	II D	Remolded	276	13.3	790.2
C	8	II D	Remolded	138	11.7	437.3
C	9	II D	Remolded	207	11.7	664.7

Table 6: Drained shear strength parameters of saprock from the weathering profile.

Set	Samples	Sub-zone (Mass Weathering Grade)	Vertical Depth (m)	Cohesion (c') (kPa)	Angle of Friction (φ')
Set A	1, 2 & 3	II B (V)	16.11 m	30.6	33.2
Set B	4, 5 & 6	II C (IV)	20.86 m	19.5	31.4
Set C	7, 8 & 9	II D (III)	31.29 m	20.2	34.4
All	All	Saprock (III - V)		14.5	34.3

the drained shear strength parameters which are characterized by values of effective cohesion (c') and effective angle of internal friction (φ') (Table 6). An example of the plots of the values of *pf* = [(σ1 + σ3)/2] and *qf* = [(σ1 - σ3)/2] and the drawing of K_f *lines* for the samples of Set A is shown in Figure 7.

Effective cohesions are somewhat variable; sets A, B and C being characterized by cohesions of 30.6, 19.5, and 20.2, kPa, respectively (Table 6). Effective friction angles, however, are less variable with sets A, B and C characterized by values of 33.2°, 31.4°, and 34.4°, respectively (Table 6). When the values of *pf* = [(σ1 + σ3)/2] and *qf* = [(σ1 - σ3)/2] for all sample sets are plotted, an overall effective cohesion of 14.5 kPa, and overall friction angle of 34.3° is calculated for the saprock (Table 6).

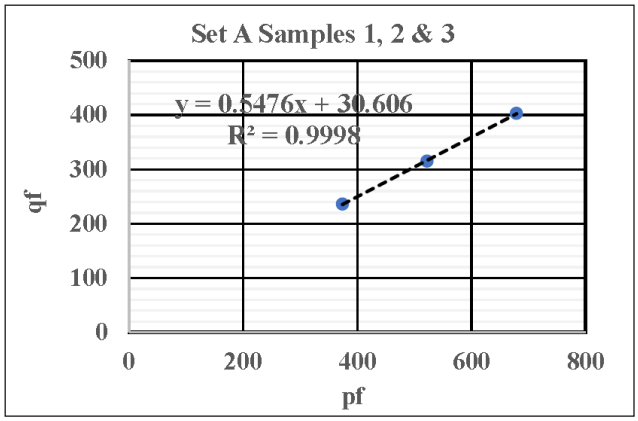

Figure 7: Example of plots of *pf* = [(σ1 + σ3)/2] and *qf* = [(σ1 - σ3)/2] and drawing of K_f *lines*.

DISCUSSION

It has been earlier pointed out that there is very little published data on the drained shear strength parameters of earth materials in weathering profiles over granitic bedrock in Malaysia. The following discussion thus considers the main factors that influence the drained shear strength parameters of saprock at the investigated weathering profile.

Published results of consolidated drained triaxial tests

The effective friction angles (of 31.4° to 34.4°) determined in the present study for saprock (zone II) samples are very similar to those (of 28.0° to 32.6°) reported from published work in Malaysia (Table 7). The published work, however, involves samples collected at shallow depths in pedological soil profiles (zone I) of weathering profiles

over granitic bedrock (Mohd. Raihan *et al.*, 1998; Salih & Kassim, 2012; Salih & Ismael, 2019). Some difference in the friction angles can therefore, be expected as differences in sampling depths give rise to textural and compositional differences between samples.

The effective friction angles of the present study are very similar to those (of 27° to 38°) reported from published work in Singapore (Table 7). These results, based on multi-stage consolidated drained triaxial tests, are more relevant as they include samples from saprock (zone II) in a weathering profile over the Bukit Timah granite (Rahardjo *et al.*, 2004). Some difference in friction angles, however, is expected as there will be textural differences in samples due to differences in composition and texture of the original granitic bedrock. The multi-stage testing procedure furthermore, has not been recommended for determining the shear strength parameters of 'residual soils' as it is said to often yield misleading, high values of apparent cohesion (Tan & Gue, 2001). The multi-stage triaxial tests themselves have also been said to cause an increase in the stiffness of samples as well as a decrease in the failure strain during subsequent applications of stress (Rahardjo *et al.*, 2003).

The effective cohesions (of 19.5 to 30.6 kPa) determined in the present study are not comparable with those (of 8.0 to 10.0 kPa) reported from published work in Malaysia (Table 7). These differences are not unexpected as there are textural and compositional differences; the samples of the present study from saprock (zone II) and those of published work from the pedological soil profile (zone I) (Mohd. Raihan *et al.*, 1998; Salih & Kassim, 2012; Salih & Ismael, 2019).

The effective cohesions of the present study are comparable with those (of 12.0 to 26.0 kPa) reported in the published work from Singapore (Table 7) which are more relevant as they involve samples from saprolite (sub-zone I C) and saprock (zone II) (Rahardjo *et al.*, 2004). Differences in effective cohesions, however, are expected as there are textural and compositional differences in the original granitic bedrocks. Concerns have also been expressed on the multi-stage testing procedure employed for determination of the drained shear strength parameters (Tan & Gue, 2001; Rahardjo *et al.*, 2003).

Effective friction angle of saprock (zone II) samples

The drained strength parameters of all sample sets are characterized by moderate values of the effective friction angle, ranging from 31.4° to 34.4°, with an average angle of 34.3° (Table 6). These friction angles show little correlation with physical properties of the saprock as density and porosity; linear regression analyses yielding low R-squared values (<0.5000). The friction angles, however, distinctly increase with an increase in sand contents (R^2=0.9855), as well as sand and gravel contents (R^2=0.8528) (Figures 8 and 9). This increase in friction angles is not unexpected for increasing sand and gravel contents will increase inter-locking and thus resistance to displacement (during shear) amongst the coarse particles. The coarse particles mainly consist of angular quartz grains that have become disaggregated, individual particles due to *in situ* alteration of the surrounding feldspar and other mineral grains (Table 2).

Effective cohesion of saprock (zone II) samples

The drained strength parameters of all sample sets are characterized by effective cohesions ranging from 19.5 to 30.6 kPa, with an average value of 14.5 kPa (Table 6). Cohesion intercepts from triaxial tests on 'residual soils' over granitic bedrock are said to reflect the existence of bonds between particles (Tan & Gue, 2001). Several causes have been proposed for the bonds and include cementation through deposition of carbonates, hydroxides and organic

Table 7: Shear strength parameters from published consolidated drained triaxial tests.

No	Soil type	Weathering Grade (Depth)	c' (kPa)	ϕ' (°)	Comments	Reference
1	Sandy silt (Saprolite)	VI (Depth?)	10	28.1°	Granitic soil	Mohd Raihan *et al.* (1998)
2	Gravelly silt (Topsoil)	VI (1.5-2.5 m)	8 - 9	28° - 30°	Skudai, Johore	Salih & Kassim (2012)
3	Clayey gravel	VI (1.5-2.5 m)	8.13	28.17°	Remold 100 kPa	UTM Campus, Johore. Salih & Ismael (2019)
			9.04	29.79°	Remold 200 kPa	
	Silty gravel (Saprolite)	VI (3.5 m)	1.12	31.02°	Remold 100 kPa	
			1.42	32.57°	Remold 200 kPa	
4	Residual soil	General	7 - 77	17° - 40°	Literature Review	Salih (2012)
5	Sandy silt	VI (5-9 m)	26	27°	Multi-stage tests. Bt. Timah granite, Singapore	Rahardjo *et al.* (2004)
	Silty sand	V (10-15 m)	13	35°		
	Silty sand	V (15-21 m)	12	38°		

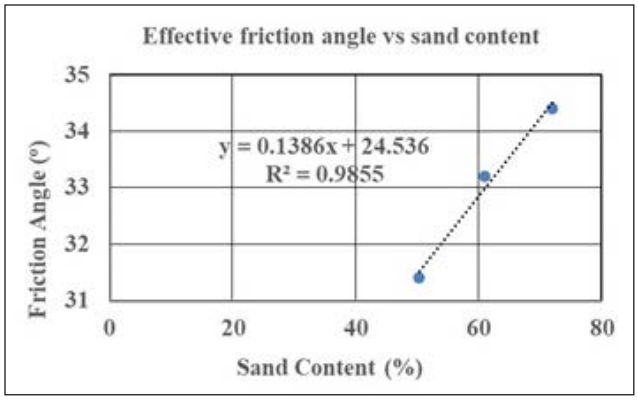

Figure 8: Effective friction angle versus sand content.

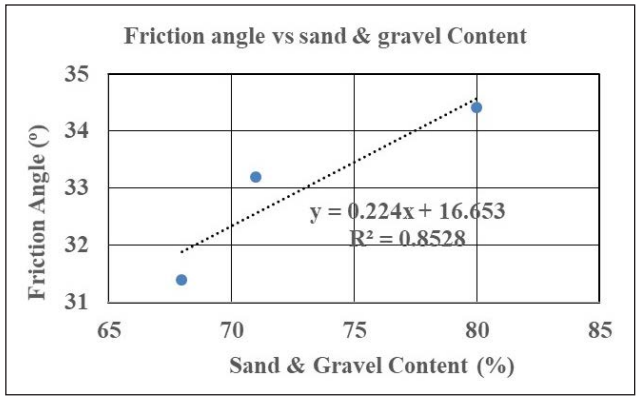

Figure 9: Effective friction angle versus sand and gravel content.

matter, pressure solution and re-precipitation of cementing agents as well as the growth of bonds during chemical alteration of minerals (Vaughn, 1988; Tan & Gue, 2001). Such bonds, however, are not expected in the samples of the present study for they (apart from one undisturbed sample) were prepared by remolding disaggregated tube samples. Remolding furthermore, has been shown to alter the relative distribution of pores in soil samples with reference to undisturbed ones (Rao & Revanasiddappa, 2005).

Linear regression analyses show little correlation (R^2 <0.5000) between effective cohesions and physical and soil index properties of saprock as density, porosity, and gravel, sand, silt and clay contents. Regression analyses, even with the limited number of samples, however, indicate increasing effective cohesions with increasing moisture contents (R^2=0.8269); a relationship that points to the influential role of moisture content (Figure 10).

Soil-moisture retention curves furthermore, show the earth materials of the weathering profile to experience increasing matric suction (or negative pore water pressures) with decreasing moisture contents (Raj, 2010). A regression analysis of the gravimetric moisture contents at pF 4.19 (1,500 kPa) suction of samples from sub-zones II B, II C and II D (Raj, 2010) versus the effective cohesions of the present study yields a distinct positive trend (R^2=0.9208) (Figure 11). In agriculture, the moisture content at pF 4.19 (1,500 kPa) suction is known as the wilting point for it is the minimum moisture content of soil that can support plant growth. Water in soil beyond pF 4.19 (1,500 kPa) suction comprises water molecules that adhere to the surfaces of soil particles and can only be removed on heating in an oven (Easton, 2016).

Even with the limited number of samples, the regression analysis (Figure 11) indicates that effective cohesions in the present study are due to negative pore water pressures (or matric suction). Matric suction in unsaturated or partly saturated soils is considered to be a most important phenomenon that enhances their shear strength; some authors considering suction to be "apparent cohesion" (Lumb, 1975; Vanapalli *et al.*, 1996; Leong *et al.*, 2001; Thamer *et al*., 2006).

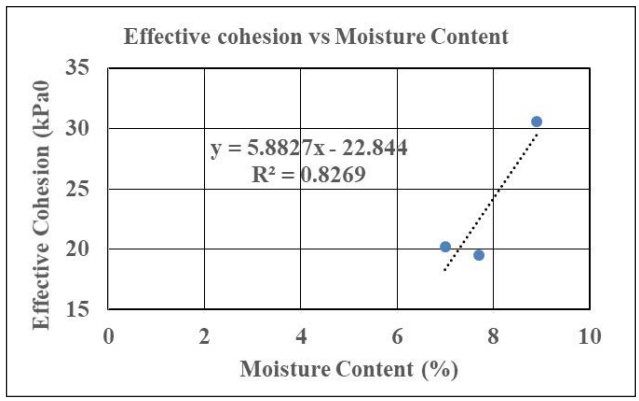

Figure 10: Effective cohesion versus moisture content.

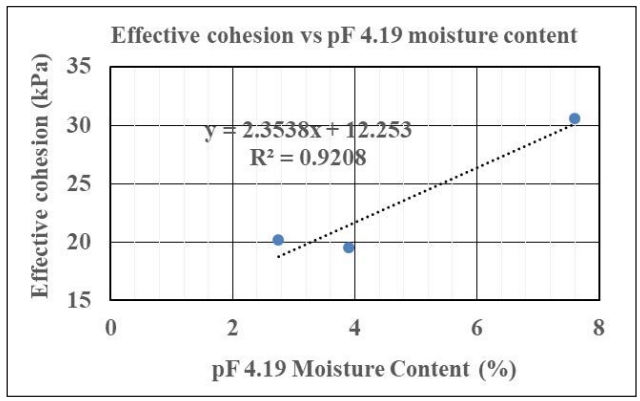

Figure 11: Effective cohesion versus moisture content at pF 4.19 (1,500 kPa) suction..

CONCLUSIONS

Three broad zones were differentiated at the weathering profile; an upper, 9.4 m thick, pedological soil (zone I), an intermediate, 31.7 m thick, saprock (zone II) and the bottom bedrock (zone III). The saprock (zone II) comprises gravelly silty sands that indistinctly to distinctly preserve the minerals, textures and structures of the original granite and can be separated into four sub-zones; II A, II B, II C and II D based on differences in preservation of relict structures and content of litho-relicts (core-boulders).

Consolidated drained triaxial tests on remolded samples of saprock from sub-zones II B, II C and II D, yield effective cohesions (c') of 30.6 kPa, 9.5 kPa, and 20.2 kPa, and effective friction angles of 33.2°, 31.4° and 34.4°, respectively. Regression analyses show these strength parameters to have little correlation with most physical and soil index properties of the saprock as density and porosity, as well as silt and clay contents.

Regression analyses furthermore, show increasing effective cohesions with increasing moisture contents retained at pF 4.19 (1,500 kPa) suction; a feature reflecting the influence of negative pore water pressures (or matrix suction). Regression analyses also show increasing friction angles with increasing sand, and sand and gravel, contents; features that reflect increased inter-locking and resistance to displacement of the coarse grained particles during shear.

It is concluded that the drained shear strength of saprock is characterized by an average effective cohesion of 14.5 kPa, and average friction angle of 34.3°; these parameters being influenced by the moisture contents retained at 1,500 kPa suction, and the sand and gravel contents.

ACKNOWLEDGEMENTS

Grateful thanks are extended to the Department of Civil Engineering at the Faculty of Engineering, University of Malaya for use of facilities at their Soil Mechanics Laboratory. Financial support for field and laboratory investigations in the preparation of this paper from an F Vote Research Grant by the University of Malaya is also gratefully acknowledged. Grateful thanks are also extended to the two anonymous reviewers for their valuable comments.

CONFLICT OF INTEREST

The author has no conflicts of interest to declare that are relevant to the contents of this article.

REFERENCES

Bishop, A.W., & Henkel, D.J., 1957. The measurement of soil properties in the Triaxial Test. Edward Arnold, London. 189 p.

Brand, E.W., 1982. Analysis and design in residual soils. Proceedings Conference on Engineering & Construction in Tropical & Residual Soils, ASCE, Honolulu, Hawaii, 89-129.

Dearman, W.R., 1974. Weathering classification in the characterization of rock for engineering purposes in British practice. Bulletin International Association of Engineering Geology, 9, 33-42.

Easton, Z.M., 2016. Soil and soil water relationships. College Agriculture & Life Sciences, Virginia State University, Publication BSC-194P (https://ext.vt.edu>agriculture>water). 9 p.

Faisal, H.A., Bujang B.K. Huat, & Low, T.H., 2005. Infiltration characteristics of granitic residual soil of various weathered grades. American Journal Environmental Sciences, 1, 64-68.

GSL (Geological Society of London), 1990. Tropical residual soils. Geological Society Working Group Report, Quarterly Journal Engineering Geology, 23, 1-102.

Haile, N.S., Stauffer, P.H., Krishnan, D., Lim, T.P., & Ong, G.B., 1977. Palaeozoic redbeds and radiolarian cherts: Reinterpretation of their relationships in the Bentong and Raub areas, West Pahang, Peninsular Malaysia. Bulletin of the Geological Society of Malaysia, 8, 45-60.

IAEG (International Association Engineering Geology), 1981. Rock and soil description for engineering geological mapping. Bulletin International Association of Engineering Geology, 24, 235-274.

Lambe, T.W., & Whitman, R.V., 1973. Soil mechanics. Wiley Eastern Private Ltd., New Delhi. 553 p.

Leong, E.C., Rahardjo, H., & Fredlund, D.D., 2001. Application of unsaturated soil mechanics in geotechnical engineering. Proceedings 8th East Asian Pacific Conference on Structural Engineering & Construction, Singapore, 5-7 Dec. 2001, 67 p.

Lumb, P., 1975. Slope failures in Hong Kong. Quarterly Journal Engineering Geology, 8, 31-36.

Mohd Raihan, T., Md. Kamal Hossain, Zamri Chik, & Khairul Anuar Mohd Nayan, 1998. Geotechnical behavior of a Malaysian residual granitic soil. Pertanika Journal of Science & Technology, 7(2), 151-169.

Ng, T.F., 1992. Petrography, structure and geotechnical studies of the Kuala Lumpur Granite, eastern part of Kuala Lumpur, Peninsular Malaysia. M.Phil. Thesis, Institute for Advanced Studies, University of Malaya. 527 p.

Rahardjo, H., Leong, E.C., & Rezaur, R.B., 2003. Shear strength characteristics of residual soils in Singapore. Keynote Lecture, Proceedings International Conference on Problematic Soils, Nottingham, July 28-30, 2003, United Kingdom. 12 p.

Rahardjo, H., Aung, K.K., Leong, E.C., & Rezaur, R.B., 2004. Characteristics of residual soils in Singapore as formed by weathering. Engineering Geology, 73, 157-169.

Raj, J.K., 1983. A study of residual soils and their cut slope stability in selected areas of Peninsular Malaysia. Ph.D. Thesis, Faculty of Science, University of Malaya. 462 p.

Raj, J.K., 1985. Characterization of the weathering profile developed over a porphyritic biotite granite bedrock in Peninsular Malaysia. Bulletin International Association of Engineering Geology, 32, 121-128.

Raj, J.K., 2009. Geomorphology. In: Hutchison, C.S., & D.N.K. Tan (Eds.), Geology of Peninsular Malaysia, University of Malaya and Geological Society of Malaysia, Kuala Lumpur, 5-29.

Raj, J.K., 2010. Soil moisture retention characteristics of earth materials in the weathering profile over a porphyritic biotite granite. American Journal of Geosciences, 1, 12-20.

Raj, J.K., 2021. Saturated hydraulic conductivity (Ks) of earth materials in the weathering profile over a porphyritic biotite granite in Malaysia. Bulletin of the Geological Society of Malaysia, 71, 1-8.

Rao, S.M., & Revanasiddappa, K., 2005. Role of micro-fabric in matrix suction of residual soils. Engineering Geology, 80, 60-70.

Salih, A.G., 2012. Review on granitic residual soils: Geotechnical properties. Electronic Journal Geotechnical Engineering, Bundle T, 17, 2645-2658.

Salih, A.G., & Kassim, K.A., 2012. Effective shear strength parameters of remolded residual soil. Electronic Journal Geotechnical Engineering, Bundle C, 17, 243-253.

Salih, A,G., & Ismael, A,M., 2019. Influence of clay contents on drained shear strength parameters of residual soil for slope stability evaluation. International Journal of Geotechnical Construction Materials & Environment (GEOMATE), 17(59), 166-172.

Tan, Y.C., & Gue, S.S., 2001. The determination of shear strength in residual soils for slope stability analysis. Proceedings Seminar Cerun Kebangsaan 2001, Cameron Highlands, 14-15 May 2001, 1-18.

Thamer, A.M., Faisal Hj. Ali, S. Hashim, & Bujang B.K. Huat, 2006. Relationship between shear strength and soil water characteristic curve of an unsaturated granitic residual soil. American Journal Environmental Sciences, 2 (4), 142-145.

Thomas, M.F., 1974. Tropical geomorphology - A study of weathering and landform development in warm climates. Macmillan Press Limited, London. 332 p.

Vanapalli, S.K., Fredlund, D.D., & Clifton, A.W., 1996. Model for the prediction of shear strength with respect to soil suction. Canadian Geotechnical Journal, 33(3), 379-392.

Vaughan, P.R., 1988. Characterizing the mechanical properties of *in situ* residual soil. Keynote Paper, Proceedings Second International Conference on Geomechanics in Tropical Soils, Singapore, 2, 469-487.

Wesley, L., 2009. Behaviour and geotechnical properties of residual soils and allophone clays. Obras y Proyectos, 6, 5-10.

Manuscript received 21 December 2020;
Received in revised form 26 June 2022;
Accepted 5 July 2022
Available online 30 November 2022